

<https://doi.org/10.33472/AFJBS.6.2.2024.477-495>



African Journal of Biological Sciences



Research Paper

Open Access

Possible Role of FDG PET/CT in Diagnosis and Staging of Recurrent Ovarian Cancer

Hoda Fatouh Ahmad Lotfy, Inas Mohamed Abdelaziz Elfiki, Maged Abdelgalil Hamed, Mona Mahmoud Eladl

Radiodiagnosis Department, Faculty of Medicine, Zagazig University, Egypt

Dr.Hodafatouh@gmail.com

Article History

Volume 6, Issue 2, April 2024

Received: 19 April 2024

Accepted: 6 May 2024

Published: 16 May 2024

doi: 10.33472/AFJBS.6.2.2024.477-495

Abstract: Ovarian cancer is the second most frequent gynecologic malignancy (preceded by cervix carcinoma) with up to 25 and 75 % chance of 2 years' recurrence of early and advance stages respectively. PET is a tomographic scintigraphic technique in which a computer-generated image of local radioactive tracer distribution in tissues is produced through the detection of annihilation photons that are emitted when radionuclides introduced into the body decay and release positrons. 18F-FDG PET is a tomographic imaging technique that uses a radiolabeled analog of glucose, 18F-FDG, to image relative glucose use rates in various tissues. Because glucose use is increased in many malignancies, 18F-FDG PET is a sensitive method for detecting, staging, and monitoring the effects of therapy of many malignancies. CT is a tomographic imaging technique that uses an x-ray beam to produce anatomic images. This anatomic information is used to detect and to help determine the location and extent of malignancies. Combined PET/CT devices provide both the metabolic information from 18F-FDG PET and the anatomic information from CT in a single examination. Ovarian cancer is the fifth leading cause of cancer death among women in the United States and has a high likelihood of recurrence despite aggressive treatment strategies. Detection and exact localization of recurrent lesions are critical for guiding management and determining the proper therapeutic approach, which may prolong survival. Because of its high sensitivity and specificity compared with those of conventional techniques such as computed tomography (CT) and magnetic resonance (MR) imaging, fluorine 18 fluorodeoxyglucose positron emission tomography (PET) combined with CT is useful for detection of recurrent or residual ovarian cancer and for monitoring response to therapy. However, PET/CT may yield false-negative results in patients with small, necrotic, mucinous, cystic, or low-grade tumors. In addition, in the posttherapy setting, inflammatory and infectious processes may lead to false-positive PET/CT results. Despite these drawbacks, PET/CT is superior to CT and MR imaging for depiction of recurrent disease.

Keywords: FDG PET/CT, Recurrent Ovarian Cancer

Introduction: Ovarian cancer is the second most common gynecologic malignancy (after cervical cancer), with a lifetime risk of 1.7%. Although its incidence has decreased slightly over the past 30 years, it currently is the most common cause of death among women with gynecologic malignancy (1). Cytoreductive surgery, followed by paclitaxel therapy and platinum-based cytotoxic chemotherapy, is the mainstay of primary treatment for high-grade early- and advanced-stage disease (2,3). Despite high clinical response rates after optimal debulking surgery and combination chemotherapy, 50%–75% of patients still experience disease relapse (2–6). However, due to the recent emergence of alternative targeted therapies, which are designed to manage small-volume recurrent disease, positron emission tomography (PET) combined with computed tomography (CT) may play an important role in early detection of recurrent ovarian cancer. Serum CA-125 assay, physical examination, and anatomic imaging have been widely used to evaluate patients with ovarian cancer. Use of these methods is associated with limited success, and currently there is no agreement on which type of follow-up examination should be used or when it should be employed (7,8).

Potential advantages of the use of integrated PET/CT for evaluation of recurrent ovarian cancer include increased lesion detection with the use of a metabolic tracer, simultaneous acquisition of anatomic reference points to determine the exact location of lesions, and, in most cases, differentiation of disease processes from physiologic processes (9). Moreover, PET/CT may be used to survey the entire body. These superior qualities may help identify which patients are eligible for secondary surgical cytoreduction; however, further investigation with prospective, randomized trials that examine various therapeutic interventions on the basis of PET/CT results is warranted (10).

In this article, the characteristics and patterns of spread of recurrent ovarian cancer and the strengths and limitations of PET/CT for the detection of disease relapse are discussed. Multiple case examples are presented, with contrast material-enhanced CT juxtaposed with PET/CT for comparison purposes.

Ovarian Cancer

In 75% of cases of ovarian cancer, the patients have advanced-stage disease at the time of diagnosis, a result of its late and insidious onset of symptoms (10). In stage I disease, tumor is limited to the ovaries; in stage II, it extends into the pelvis; in stage III, it spreads beyond the pelvis; and in stage IV, it involves distant sites such as the liver parenchyma (11). The 5-year survival rate for patients with stage I disease is 90%; this rate decreases to 25% for those with distant metastases (2).

Surgery is the cornerstone of management of epithelial ovarian cancer, with broad applications throughout the clinical course of disease, from the patient's initial diagnosis to palliative care.

Comprehensive surgical staging is essential for precise prognostic determination and treatment planning for patients with apparent early-stage ovarian cancer. After primary

cytoreductive surgery, adjuvant chemotherapy is administered, usually a combination of paclitaxel and platinum-based compounds (12).

After primary surgery and chemotherapy, the National Comprehensive Cancer Network guidelines recommend that disease status be monitored with regular physical and pelvic examinations, contrast-enhanced CT, magnetic resonance (MR) imaging, fluorine 18 fluorodeoxyglucose (FDG) PET/CT, and measurement of serum CA-125 levels (13).

Ovarian cancer-associated antigen CA-125, also known as mucin 16, is part of the mucin family glycoproteins (14). In patients with elevated CA-125 levels that normalize after chemotherapy, two consecutive measurements of elevated CA-125 levels are indicative of recurrent epithelial ovarian cancer, even in the absence of clinical or radiologic findings (15–17). Convincing data suggest that persistently rising serum CA-125 levels provide strong evidence for progressive ovarian cancer. CA-125 is neither specific for ovarian cancer nor sensitive for small-volume disease; approximately 20% of all ovarian cancers are negative for CA-125 expression (17). The baseline CA-125 level before initiation of maintenance chemotherapy is indicative of the risk for subsequent relapse. Despite high positive predictive values (>95%) associated with CA-125, its negative predictive value is low, at 50%–60% (18,19). Therefore, CA-125 is useful when levels are elevated, but normal values do not exclude the possibility of recurrence.

With appropriate surgical selection criteria, secondary cytoreduction surgery may substantially prolong survival in patients with recurrent ovarian cancer (12). The success of additional chemotherapy and external radiation therapy largely depend on the extent of disease (12,20). Overall, improved diagnostic methods are needed to better estimate tumor load and residual disease and to quantify the volume of disease and of ascites, which may serve as better surrogate markers for response to therapy (21).

Patterns of Spread of Ovarian Cancer Ovarian cancer usually spreads to the local lymph nodes, implants on the peritoneum by way of lymphatic channels, or, less frequently, disseminates hematogenously (20). In patients with ovarian cancer, the most common histologic subtypes of peritoneal carcinomatosis are serous papillary carcinoma and poorly differentiated adenocarcinoma (22,23). Tumor cells that continuously invade the peritoneal cavity usually shed into the intraperitoneal fluid, which continuously circulates through the abdomen and transports the deposits of malignant tumor cells. Common sites of implantation are the pelvis, right hemidiaphragm, liver, right paracolic gutter, bowel, and omentum. Transdiaphragmatic spread to the pleura is common in patients with ovarian cancer (24).

Lymph node involvement at primary surgery has a reported incidence of 25% in patients with stage I disease; 50%, stage II disease; and 74%, stage III–IV disease (25). Among

patients with peritoneal metastases, approximately 30% have visceral or extraperitoneal metastases involving pelvic, paraaortic, or inguinal lymph nodes.

Imaging of Recurrent Ovarian Cancer Early detection of recurrent disease is important for proper treatment selection (7). Metastases from ovarian cancer primarily involve the peritoneum rather than parenchymal sites; thus, the presence of small-volume recurrence or metastatic deposits on the visceral surfaces poses a challenge for interpretation of CT and MR images (23,26). In addition, after surgery, anatomic structures may appear distorted, resulting in equivocal or inaccurate imaging findings. Spiral CT usually has a sensitivity of 85%–93% for the detection of large peritoneal metastases; however, this sensitivity decreases to 25%–50% for those with a diameter less than 1 cm (23,26).

A recent meta-analysis reported that for the detection of recurrent disease, the overall diagnostic ability of CT was similar to that of MR imaging (27–33). However, MR imaging has inherent advantages over CT that are related to safety issues: MR imaging uses no ionizing radiation and the contrast agents used for MR imaging have fewer side effects than those used for CT (34,35).

FDG PET/CT has a reported sensitivity of 80%–100% for the detection of recurrent ovarian cancer (9). The spatial resolution of PET is approximately 6–10 mm; therefore, its sensitivity for depicting lesions smaller than 1 cm is lower than that for larger lesions (36). Subcentimeter lesions of omental carcinomatosis may not demonstrate sufficient radiotracer uptake, even if infiltrative changes indicative of the presence of disease are seen at CT (37). The reported specificity of PET for the detection of recurrent ovarian cancer ranges from 42% to 100% (9,36–39). A paucity of data exists regarding the comparison of PET with MR imaging for detection of ovarian cancer recurrence. In patients with ovarian cancer who had undergone cytoreductive surgery, MR imaging appears to have higher sensitivity for detection of recurrent peritoneal metastases within the pelvis, although PET/CT has slightly higher specificity. PET/CT has a patient-based sensitivity and specificity of 73% and 91%, respectively, for detection of such metastases, and the corresponding values for MR imaging are 93% and 86%, respectively. PET/CT and MR imaging have lesion-based sensitivity of 43% and 86%, respectively (39).

A progressive rise in serum tumor marker CA-125 is an early indication of recurrent epithelial ovarian cancer. However, elevated CA-125 titers are not always specific for malignancy (15–18). Zimny et al (40) reported that PET has a sensitivity of 96% for localizing recurrent disease in patients with rising CA-125 levels. PET evidence of recurrent ovarian cancer preceded CT findings by 6 months, allowing earlier reintroduction of therapy. Other investigators corroborated these findings, reporting that a combination of FDG PET and CA-125 tumor marker yields a sensitivity of 94%–98%, whereas conventional imaging results are negative or equivocal (32,41–43).

Patient-based analysis of the accuracy of PET combined with contrast-enhanced CT compared with PET combined with low-dose CT and contrast-enhanced CT alone for the

detection of suspected recurrent ovarian cancer revealed that the sensitivity and specificity of PET combined with contrast-enhanced CT were 79% and 91%, respectively, compared with 74% and 91% for PET combined with low-dose CT and 61% and 85% for contrast-enhanced CT alone (39).

In a meta-analysis by Gu et al (33), the area under the receiver operating characteristic (AUC) curve was 0.92 for CA-125, 0.93 for PET alone, 0.96 for PET/CT, 0.88 for CT, and 0.8 for MR imaging for detection of recurrent ovarian cancer. CA-125 and PET/CT had the highest pooled specificity (93%) and sensitivity (91%). According to a comparison of all modalities, the AUC value for PET, with and without integrated CT, was higher than those for CT and MR

imaging alone. However, despite the relatively high sensitivity and specificity of combined PET/CT for detection of recurrent disease, there was a substantial difference between PET results interpreted with CT and those interpreted without CT, a finding likely due to the inability of CT to localize diffuse disease involvement within the peritoneum. Because of postoperative anatomic distortions, the uptake that corresponds to bowel loops may be interpreted as physiologic rather than serosal involvement unless discrete nodules are appreciated on accompanying CT images.

According to recent studies, treatment for suspected recurrent ovarian cancer may be altered on the basis of PET/CT findings in as many as 40%–60% of patients (44–46). Some authors re-

ported that combined PET and contrast-enhanced CT findings led to a change in strategy in approximately 40%–44% of patients compared with contrast-enhanced CT findings alone, which affected treatment strategy in only 12% of patients (46).

FDG PET/CT may be used to help guide the patient selection process for site-specific treatment, including radiation therapy planning, and it may aid in the selection of optimal surgical candidates. It also may depict otherwise undetected recurrent disease, regardless of the patient's CA-125 levels. There is strong evidence to support the use of FDG PET/CT in patients with suspected recurrent disease, rising CA-125 levels, and negative CT or MR imaging results for early detection of recurrent ovarian cancer (33,41–43). However, it remains to be proved whether the anatomic information provided by CT significantly improves the overall diagnostic accuracy of PET

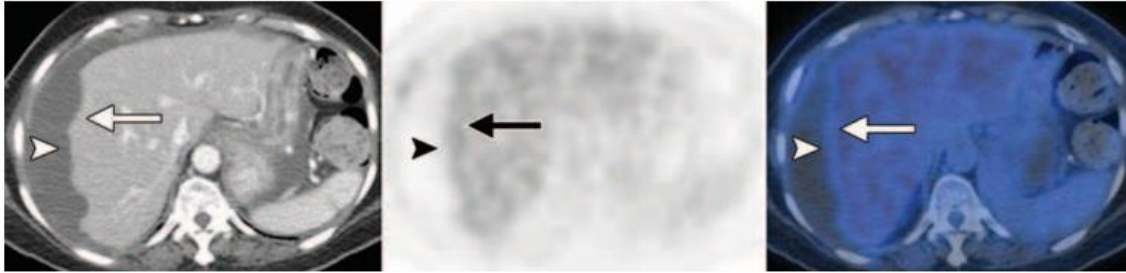


Figure 1. False-negative PET results in a 76-year-old woman with miliary peritoneal carcinomatosis, elevated CA-125 levels, and a history of total abdominal hysterectomy (TAH), bilateral salpingo-oophorectomy (BSO), omentectomy, lymph node dissection, and chemotherapy for stage IIIC ovarian mucinous cystadenocarcinoma. Axial contrast-enhanced CT (left), FDG PET (middle), and fused PET/CT (right) images show perihepatic ascites compressing the liver parenchyma (arrowhead), which is not metabolically active. Mild FDG uptake (mean maximum standardized uptake value [SUV_{max}], 2.3) similar to background liver uptake is seen along the peritoneal surface of the hepatic convexity (arrow), although CT clearly shows scalloping along the liver parenchyma, a finding indicative of peritoneal carcinomatosis. A limitation of FDG PET/CT is its inability to depict cystic or necrotic and mucinous lesions. It may also have false-negative results for small-volume disease (<7 mm) and miliary, diffuse peritoneal involvement.

PET/CT Findings of Ovarian Cancer Metastases

Peritoneal Metastases

At PET/CT, peritoneal implants appear as nodular soft-tissue masses, often with a variable degree of increased metabolic activity. Impaired lymphatic drainage of the peritoneum, a result of blocked diaphragmatic lymphatics, plays an important role in the development of ascites (Fig 1). Tumor cells tend to follow the circulatory path of peritoneal fluid, implanting in the posterior cul-de-sac (the pouch of Douglas), paracolic gutters, small bowel mesentery, ileocecal junction, diaphragmatic surface—particularly the right subphrenic space along the convexity of the liver—and hepatorenal fossa (Figs 2–4) (24). The hepatorenal fossa harbors malignant implants by communicating with the right subphrenic space and the right paracolic gutter. In almost 50% of patients, gravitational accumulation of tumor cells in the mesenteric recesses leads to seeding of malignant cells on small bowel serosal surfaces and in the ileocecal junction (24). Other sites of involvement include the sigmoid mesocolon, a result of pooling along its superior border (Fig

2c), and the right paracolic gutter, a result of cephalic flow. The right hemithorax also may be involved through its communication with the right subphrenic space. Omental thickening and nodularity with diffuse FDG uptake are indicative of omental involvement (Figs 5, 6). However, PET/CT is unable to depict small-volume disease (lesions 5–7 mm) and miliary or diffuse peritoneal involvement, even if the disease process is evident at CT (47) nodularity with diffuse FDG uptake are indicative of omental involvement (Figs 5, 6). However, PET/CT is unable to depict small-volume disease (lesions 5–7 mm) and miliary or diffuse peritoneal involvement, even if the disease process is evident at CT (47).

Umbilical metastases (Sister Mary Joseph nodules) are rare and are associated with widespread intraabdominal disease, particularly in patients with serous papillary cystadenocarcinoma (Fig 7) (48,49). This process may be secondary to retrograde lymphatic flow from the peritoneum or to venous spread of disease (50-54). The persistence of patency of fetal structures such as the urachus and paraumbilical veins may facilitate the spread of disease to the umbilicus.

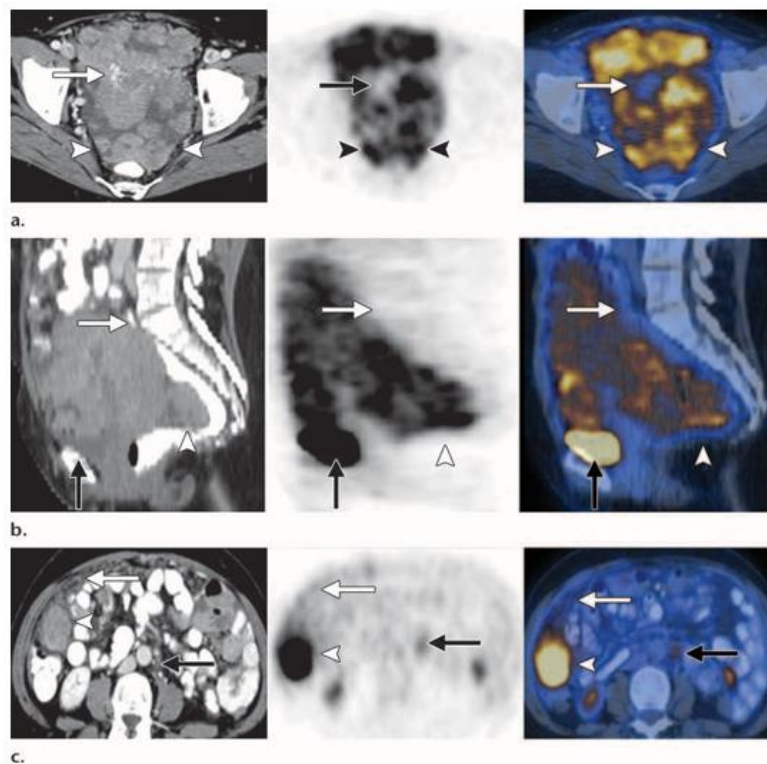


Figure 2. Peritoneal involvement in a 56-year-old woman with a history of stage IIIC serous papillary ovarian adenocarcinoma. (a) Axial contrast-enhanced high-resolution CT (left), FDG PET (middle), and fused PET/CT (right) images obtained for evaluation of disease recurrence show multiple enhancing nodules of varying sizes scattered throughout the pelvic cavity, including the cul-de-sac (arrowheads). The nodules demonstrate intense metabolic activity, a finding indicative of widespread peritoneal and mesenteric implants.

Ingested barium is seen in the markedly collapsed sigmoid colon (arrow), a result of serosal invasion. (b) Sagittal contrast-enhanced CT (left), FDG PET (middle), and fused PET/CT (right) images show the pelvic cavity and lower abdomen, which are packed with peritoneal tumor implants. The urinary bladder is seen in the lower anterior pelvic cavity (black arrow). Arrowhead = cul-de-sac, white arrow = sigmoid colon. (c) Axial CT (left), FDG PET (middle), and fused PET/CT (right) images of the abdomen show an intensely hyper-metabolic lobular enhancing mass in the right paracolic gutter (arrowhead), a finding indicative of recurrent disease. Peritoneal carcinomatosis demonstrates no appreciable increased FDG uptake (white arrow), a false-negative result most likely due to its small size and diffuse pattern of infiltration. A mildly hypermetabolic paraaortic lymph node (black arrow) also is noted and is suggestive of metastasis, although it is normal in size according to CT criteria.

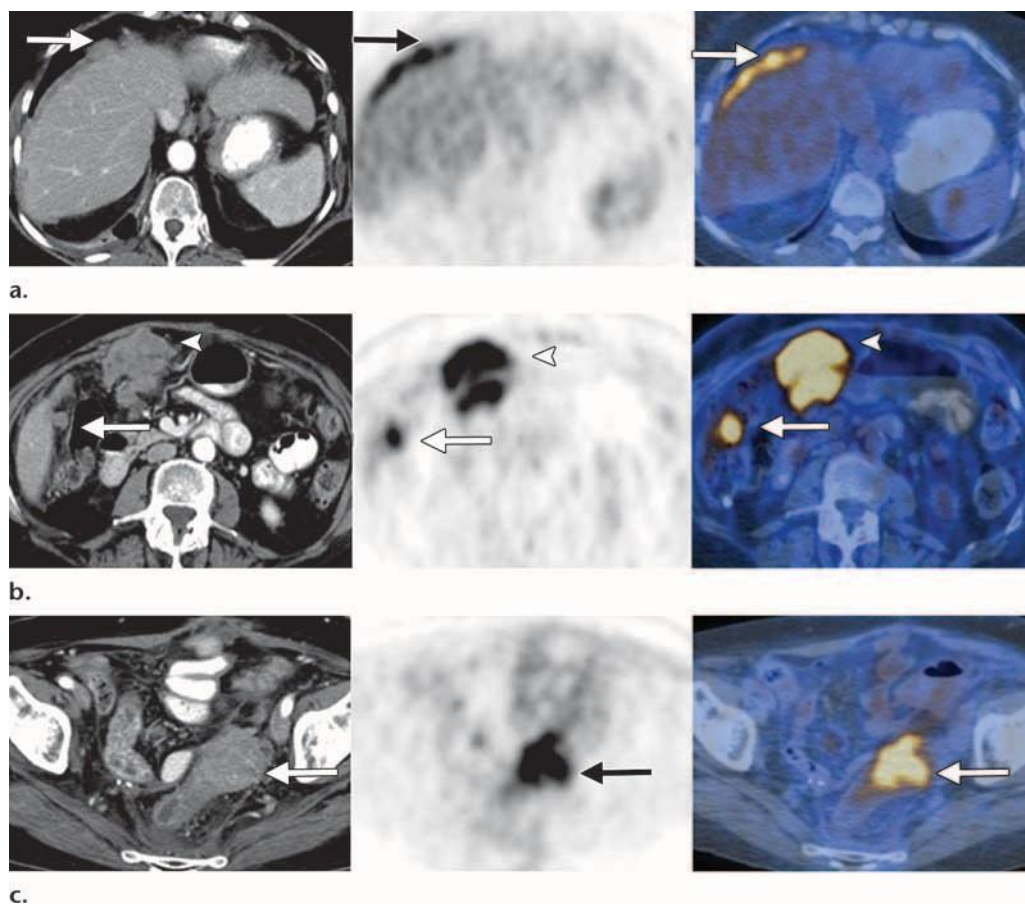


Figure 3. Peritoneal involvement in a 73-year-old woman with elevated CA-125 levels and a history of surgery and chemotherapy for stage IIIC ovarian serous papillary adenocarcinoma. **(a)** Axial contrast-enhanced CT (left), FDG PET (middle), and fused PET/CT (right) images obtained for restaging show irregular soft-tissue infiltration (arrow) in the subphrenic space along the liver convexity with markedly increased FDG uptake, a finding indicative of peritoneal tumor implants. **(b)** Axial contrast-enhanced CT (left), FDG PET

(middle), and fused PET/CT (right) images (obtained at a lower level) show a large, conglomerate, heterogeneously enhancing peritoneal mass (arrow) that demonstrates markedly increased FDG uptake throughout the peritoneum in the right side of the abdomen. An additional hypermetabolic nodular tumor deposit is seen in the subhepatic region (arrowhead). **(c)** Pelvic axial contrast-enhanced CT (left), FDG PET (middle), and fused PET/CT (right) images show an irregular enhancing mass (arrow) with markedly increased FDG accumulation in the distal sigmoid colon, a finding indicative of serosal tumor implants. The patient subsequently underwent chemotherapy; however, disease progressed over the next 2 months.

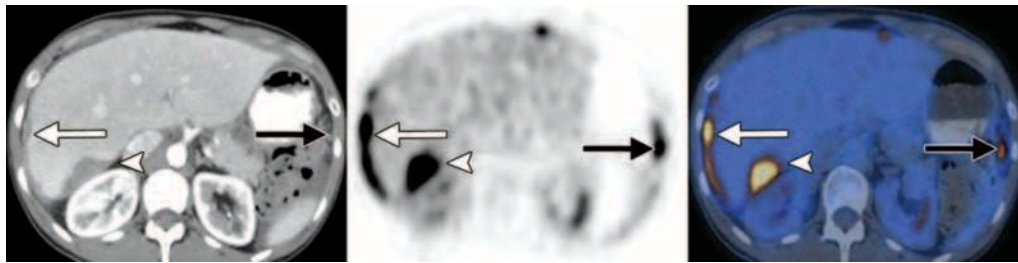
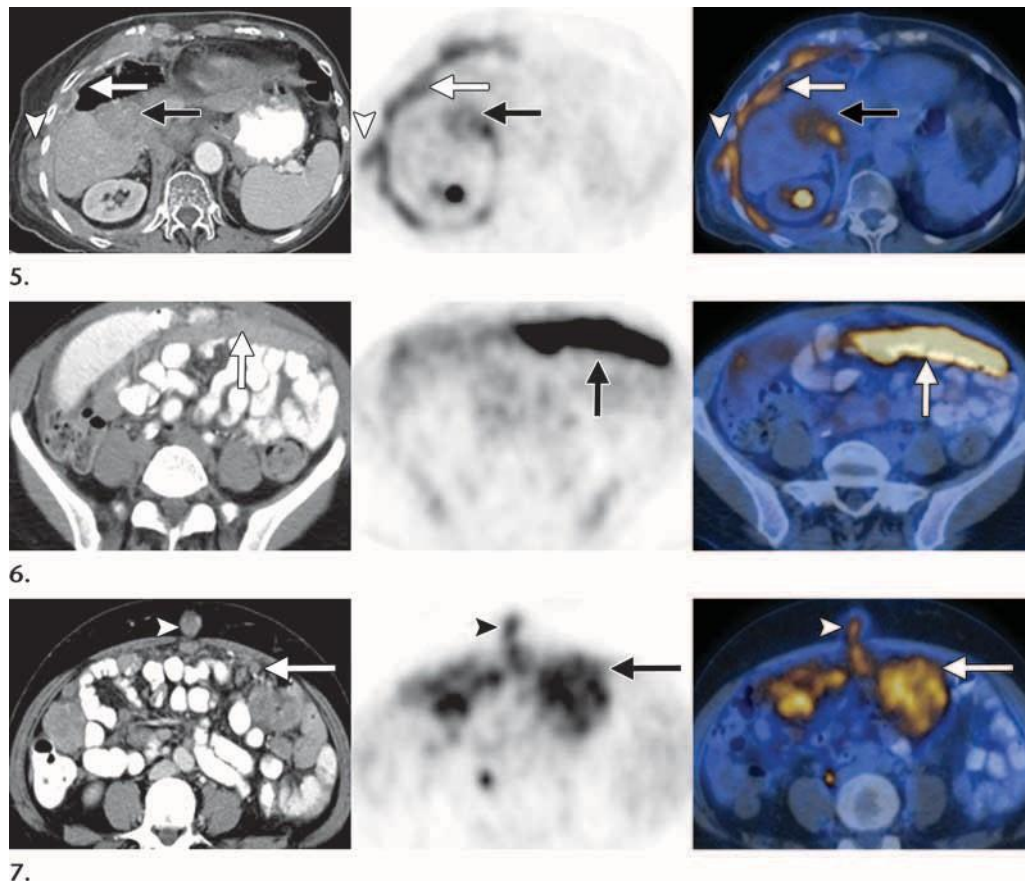


Figure 4. Peritoneal involvement in a 55-year-old woman with rising CA-125 levels and a history of surgery and adjuvant chemotherapy 7 years ago for stage IIIC ovarian serous papillary adeno- carcinoma. AXial contrast-enhanced CT (left), FDG PET (middle), and fused PET/CT (right) images obtained for disease restaging and localization show a large markedly hypermetabolic mass (arrowhead) in the hepatorenal fossa, a finding indicative of peritoneal implants. Other hypermetabolic lesions suggestive of peritoneal involvement are seen along the liver surface (white arrow) and left paracolic gutter (black arrow). Due to its diffuse nature of peritoneal involvement and the small nodular pattern, which renders the disease sites unmeasurable, peritoneal seeding may be difficult to identify at conventional imaging.



Figures 5–7. (5) Pleural and diaphragmatic involvement in a 67-year-old woman with elevated CA-125 levels and a history of debulking surgery and chemotherapy for stage II serous papillary cystadenocarcinoma. Axial contrast-enhanced CT (left), FDG PET (middle), and fused PET/CT (right) images show diffuse thickening of the pleura (white arrow) with partial calcification and increased metabolic activity. More medially, a large irregular enhancing mass lesion (black arrow) that demonstrates heterogeneous FDG uptake is seen in the diaphragm and subphrenic space (at right). A hypermetabolic nodule (arrowhead) also is seen in the right side of the chest wall, a finding indicative of chest wall invasion. The right hemithorax may be involved due to its communication with the right subphrenic space. PET/CT may be used to help detect additional sites of disease involvement that may otherwise go unnoticed. (6) Omental involvement in a 49-year-old woman with markedly elevated CA-125 levels who underwent surgery and chemotherapy for stage II ovarian serous papillary adenocarcinoma 7 months ago. Axial contrast-enhanced CT (left), FDG PET (middle), and fused PET/CT (right) images show a linear hypermetabolic lesion (arrow), which appears as mildly enhancing diffuse nodular omental thickening (a finding referred to as “omental cake”), in the anterior abdomen, a characteristic finding of omental involvement. (7) Metastasis to the umbilicus in a 56-year-old woman with rising CA-125 levels and a history of TAH, BSO, debulking surgery, and adjuvant chemotherapy 1 year ago

for stage IIIC serous papillary adenocarcinoma. Axial contrast-enhanced CT (left), FDG PET (middle), and fused PET/CT (right) images obtained for restaging show a hypermetabolic heterogeneous nodule (arrowhead) in the umbilicus contiguous with peritoneal implants, a finding indicative of a Sister Mary Joseph nodule. A markedly hypermetabolic peritoneal mass (arrow) is seen in the left side of the abdomen with slight misregistration between CT and PET/CT images due to bowel movement and respiration. Results of histopathologic analysis were positive for peritoneal metastases.

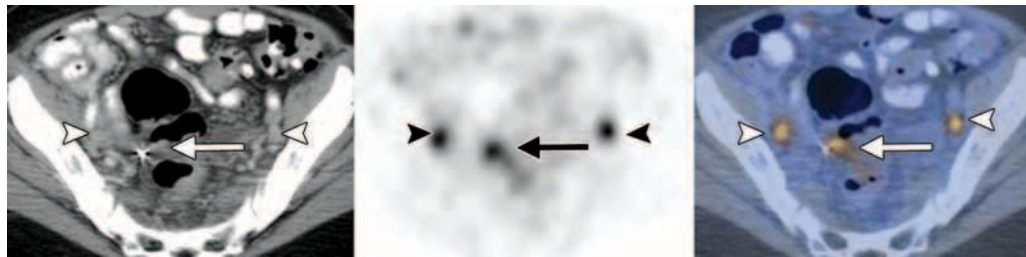


Figure 8. Lymph node metastasis in a 68-year-old woman with elevated CA-125 levels and a history of TAH, BSO, and chemotherapy for stage IIIC ovarian clear cell carcinoma. Axial contrast-enhanced CT (left), FDG PET (middle), and fused PET/CT (right) images show subcentimeter enhancing bilateral external iliac lymph nodes (arrowheads) that demonstrate increased metabolic activity, a finding indicative of lymph node involvement. An additional focus of hypermetabolic activity (arrow) is seen adjacent to a surgical clip, a finding suggestive of local recurrence. Note that the CT image does not show a definitive mass lesion next to the surgical clip, a finding probably due to the small size of the mass and the presence of metallic artifacts. Results of subsequent pelvic washing were positive for malignant cells. PET/CT may help detect residual or recurrent disease in the posttherapy setting when CT results are inconclusive due to anatomic distortion or the presence of metallic artifacts.



Figure 9. Lymph node metastasis in the same patient as Figure 8. Axial contrast-enhanced CT (left), FDG PET (middle), and fused PET/CT (right) images, obtained at the level of the thorax, show an enlarged hypermetabolic right internal mammary lymph node (arrow), a finding indicative of metastatic nodal disease. A small pleural effusion that demonstrates no metabolic activity is seen at right, a nonspecific finding.

Lymph Node Metastases

Lymphatic dissemination to the pelvic and para-aortic lymph nodes is common, particularly in patients with advanced disease (Fig 8). Spread of disease through the lymphatic channels of the

retroperitoneal lymph nodes and diaphragm may lead to dissemination into the supraclavicular or superior mediastinal lymph nodes and pleural space or, rarely, the internal mammary lymph nodes (Figs 9, 10) (23). Furthermore, involvement of the rectosigmoid colon by ovarian carcinoma

is associated with a high incidence of mesenteric nodal metastasis (Fig 11) (51). Lymph node metastasis is present in 10%–20% of patients with presumed early-stage ovarian cancer, and it is present in 40%–70% of patients with advanced-stage disease. In general, due to its low negative predictive value, pelvic PET/CT may not be used to reliably determine the likelihood of metastasis to the paraaortic lymph nodes, a finding known as a skip metastasis, which may occur in as many as 60% of patients (52–55). The reported sensitivities of CT and MR imaging for depiction of lymph node involvement are suboptimal due to the difficulty in differentiating nodal metastases from inflammatory adenopathy and fibrotic change (59). However, the performance of FDG PET is inferior, with a sensitivity of less than 50%. This suboptimal sensitivity may be attributed to the renal clearance of FDG through the ureters or into the urinary bladder, which masks nearby lymph node metastases (56–58). However, FDG PET/CT may still accurately depict metastatic disease on the basis of significantly increased metabolic activity, even in normal-sized nodes (Figs 12, 13). Notably, for detection of small or necrotic lymph nodes or early nodal involvement, evaluation with PET/CT is limited, with high false-negative rates (59-63).

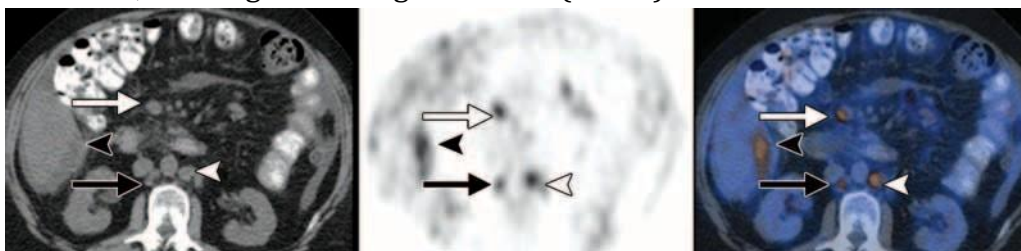


Figure 10. Lymph node metastasis in a 76-year-old woman with elevated CA-125 levels and a history of surgery and chemotherapy for stage IIIC ovarian serous papillary adenocarcinoma. Axial contrast-enhanced CT (left), FDG PET (middle), and fused PET/CT (right) images obtained for restaging show multiple enlarged hypermetabolic mesenteric lymph nodes (white arrow), paraaortic lymph nodes (white arrowhead), and an 8-mm hypermetabolic aortocaval lymph node (black arrow), findings indicative of metastatic nodal disease. A fluid collection in the hepatorenal fossa (black arrowhead) also demonstrates a linear irregular pattern of FDG uptake, a finding indicative of peritoneal implants.

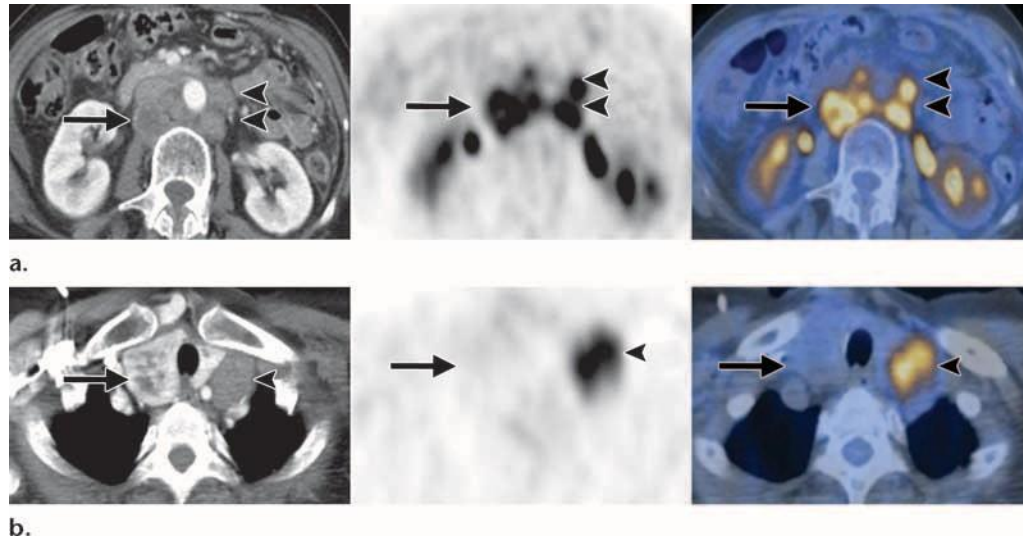


Figure 11. Lymph node metastasis in a 59-year-old woman with gradually rising CA-125 levels who underwent chemotherapy for stage IV ovarian cancer. **(a)** Axial contrast-enhanced CT (left), FDG PET (middle), and fused PET/CT (right) images show multiple enlarged paraaortic (arrowheads), aortocaval, and retrocaval (arrow) lymph nodes, all of which demonstrate markedly increased FDG uptake, a finding indicative of metastatic nodal disease. An enlarged retrocaval node with a photopenic center is noted at PET/CT, a finding that corresponds to the area of necrosis seen at CT. **(b)** Axial contrast-enhanced CT (left), FDG PET (middle), and fused PET/CT (right) images, obtained at the level of the upper thorax, show a large hypermetabolic left supraclavicular, superior mediastinal lymph node (arrowhead) compressing the left lobe of the thyroid gland, a finding indicative of distant metastatic disease. Note the enlarged and heterogeneously enhancing, nonhypermetabolic right thyroid lobe (arrow), a finding that likely is consistent with multinodular goiter.

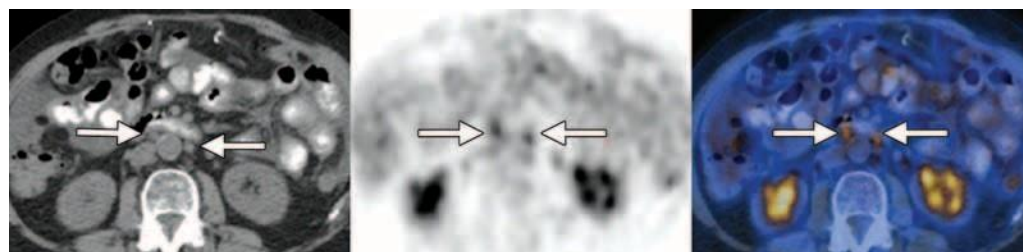


Figure 12. Normal-sized, FDG-avid metastatic lymph nodes in a 61-year-old woman with markedly elevated CA-125 levels and a history of TAH, BSO, omentectomy, and chemotherapy for stage IIIC serous papillary adenocarcinoma. Axial contrast-enhanced CT (left), FDG PET (middle), and fused PET/CT (right) images show increased FDG uptake

(SUVmax, 4.2) in multiple small paraaortic lymph nodes (arrows), some as large as 4 mm, a finding indicative of nodal metastatic disease.

e



Figure 13. Normal-sized, FDG-avid metastatic lymph nodes in a 66-year-old woman with elevated CA-125 levels and a history of surgery and chemotherapy for stage IIIC serous papillary adenocarcinoma. Axial contrast-enhanced CT (left), FDG PET (middle), and fused PET/CT (right) images show a 7-mm FDG-avid (SUVmax, 5.0) right inguinal lymph node (arrow) that was determined to be a metastatic node at subsequent biopsy.

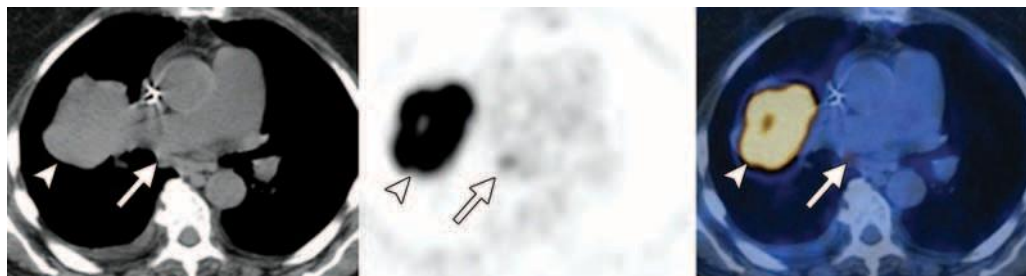


Figure 14. Distant organ metastases in an 89-year-old woman with elevated CA-125 levels and a history of surgery and chemotherapy for stage IIIC ovarian serous papillary adenocarcinoma. Axial contrast-enhanced CT (left), FDG PET (middle), and fused PET/CT (right) images show a large lobular mass (arrowhead) with a photopenic center in the right upper lobe that demonstrates markedly increased FDG uptake, a finding indicative of distant organ metastasis. A mildly hypermetabolic subcarinal lymph node (arrow) and a nonhypermetabolic small right pleural effusion are noted; however, these are nonspecific findings and may be either malignant or benign.

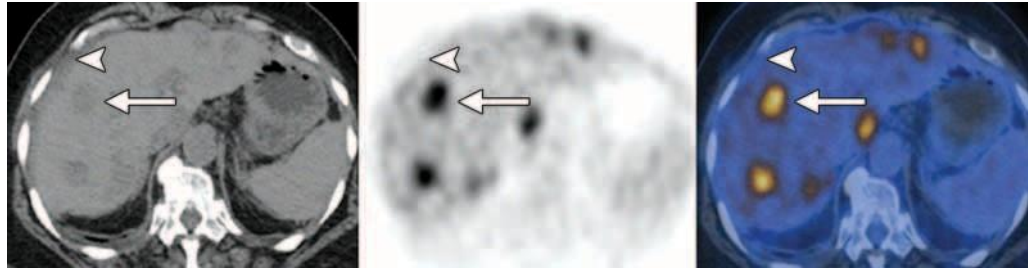


Figure 15. Distant organ metastases in a 73-year-old woman with persistently elevated CA-125 levels and a history of TAH, BSO, radical debulking surgery, and chemotherapy 6 months ago for stage IIIC serous papillary adenocarcinoma. Axial contrast-enhanced CT (left), FDG PET (middle), and fused PET/CT (right) images show multiple hypermetabolic foci throughout the liver that correspond to ill-defined hypointense hepatic masses (arrow), a finding indicative of distant organ metastases. Mild soft-tissue infiltration (arrowhead) is seen along the liver surface with no appreciable FDG uptake, a finding highly suggestive of peritoneal seeding.

Pitfalls of PET/CT

The main pitfalls of the use of PET/CT for staging of recurrent ovarian cancer include the normal physiologic activity in the bowel loops; focal retained activity in the urinary system; FDG uptake within atherosclerotic plaque; and misalignment due to bowel peristalsis, bladder filling, or diverticulitis (64-66). To avoid misinterpretation, it is important for radiologists and clinicians to recognize that PET/CT is unable to depict small-volume disease as well as diffuse, miliary peritoneal involvement. False-negative FDG PET/CT results may also occur in patients with cystic or necrotic lesions or lesions with copious mucinous collections (Fig 18). Knowledge of prior surgeries and their complications is essential to properly interpret PET images. Asymmetric FDG uptake along the surgical bed is common and may mimic malignancy; caution should be exercised when studies are interpreted within 6 months of surgery (67).

Conclusions

In the posttherapy setting, studies to date have demonstrated that PET/CT is most useful for evaluation of patients with rising serum CA-125 levels or with negative or inconclusive CT or MR imaging results. In addition, PET/CT is able to depict disease recurrence in the absence of elevated CA-125 levels. FDG PET/CT may fail to depict diffuse peritoneal disease and cystic, necrotic, or mucinous lesions. There is evidence that the additional anatomic information provided by CT improves the diagnostic accuracy of PET. Thus, it is unlikely that any one modality will ultimately replace another; rather, the combined information obtained from multiple modalities will substantially increase the ability of radiologists to identify recurrent disease. Recognizing FDG PET/CT characteristics of disease spread and recurrence, as well as common pitfalls of the use of PET/CT, will increase interpretation accuracy and help improve subsequent therapy decisions.

References:

1. Jemal A, Siegel R, Ward E, Hao Y, Xu J, Thun MJ. Cancer statistics: 2009. *CA Cancer J Clin* 2009;59 (4):225–249.
2. Aabo K, Adams M, Adnitt P, et al. Chemotherapy in advanced ovarian cancer: four systematic meta-analyses of individual patient data from 37 randomized trials. *Advanced Ovarian Cancer Trialists' Group. Br J Cancer* 1998;78(11):1479–1487.
3. Chemotherapy for advanced ovarian cancer. *Advanced Ovarian Cancer Trialists Group. Cochrane Database Syst Rev* 2000;(2):CD001418.
4. Berek JS, Tropé C, Vergote I. Surgery during chemotherapy and at relapse of ovarian cancer. *Ann Oncol* 1999;10(suppl 1):3–7.
5. International Collaborative Ovarian Neoplasm Group. Paclitaxel plus carboplatin versus standard chemotherapy with either single-agent carboplatin or cyclophosphamide, doxorubicin, and cisplatin in women with ovarian cancer: the ICON3 randomized trial. *Lancet* 2002;360(9332):505–515. [Published correction appears in *Lancet* 2003;361 (9358):706.]
6. Armstrong DK, Bundy B, Wenzel L, et al. Intraperitoneal cisplatin and paclitaxel in ovarian cancer. *N Engl J Med* 2006;354(1):34–43.
7. von Georgi R, Schubert K, Grant P, Münstedt K. Post-therapy surveillance and after-care in ovarian cancer. *Eur J Obstet Gynecol Reprod Biol* 2004;114 (2):228–233.
8. Gadducci A, Cosio S, Zola P, Landoni F, Maggino T, Sartori E. Surveillance procedures for patients treated for epithelial ovarian cancer: a review of the literature. *Int J Gynecol Cancer* 2007;17(1):21–31.
9. Pannu HK, Bristow RE, Cohade C, Fishman EK, Wahl RL. PET-CT in recurrent ovarian cancer: initial observations. *RadioGraphics* 2004;24(1): 209–223.
10. Heintz AP, Odicino F, Maisonneuve P, et al. Carcinoma of the ovary: FIGO 6th annual report on the results of treatment in gynecological cancer. *Int J Gynaecol Obstet* 2006;95(suppl 1):S161–S192.
11. Kawamoto S, Urban BA, Fishman EK. CT of epithelial ovarian tumors. *RadioGraphics* 1999;19(spec issue):S85–S102.
12. Bristow RE. Surgical standards in the management of ovarian cancer. *Curr Opin Oncol* 2000;12(5): 474–480.
13. NCCN Clinical Practice Guidelines in Oncology. National Comprehensive Cancer Network. http://www.nccn.org/professionals/physician_gls/f_guidelines.asp. Accessed February 1, 2011.
14. Yin BW, Lloyd KO. Molecular cloning of the CA125 ovarian cancer antigen: identification as a new mucin, MUC16. *J Biol Chem* 2001;276(29): 27371–27375.
15. Högberg T, Kågedal B. Long-term follow-up of ovarian cancer with monthly determinations of serum CA 125. *Gynecol Oncol* 1992;46(2):191–198.
16. Rustin GJ, Nelstrop AE, TuXen MK, Lambert HE. Defining progression of ovarian carcinoma during follow-up according to CA 125: a North Thames ovary group study. *Ann Oncol* 1996;7(4):361–364.
17. Santillan A, Garg R, Zahurak ML, et al. Risk of epithelial ovarian cancer recurrence in patients with rising serum CA-125 levels within the normal range. *J Clin Oncol* 2005;23(36):9338–9343.
18. Potter ME, Moradi M, To AC, Hatch KD, Shingleton HM. Value of serum 125Ca levels: does the result preclude second look? *Gynecol Oncol* 1989;33 (2):201–203.
19. van der Burg ME, van Lent M, Buyse M, et al. The effect of debulking surgery after induction chemotherapy on the prognosis in advanced epithelial ovarian cancer. *Gynecological Cancer Cooperative Group of the European Organization for Research and Treatment of Cancer. N Engl J Med* 1995;332 (10):629–634.
20. Amendola MA. The role of CT in the evaluation of ovarian malignancy. *Crit Rev Diagn Imaging* 1985; 24(4):329–368.

21. Petru E, Lück HJ, Stuart G, et al. Gynecologic Cancer Intergroup (GCIg) proposals for changes of the current FIGO staging system. *Eur J Obstet Gynecol Reprod Biol* 2009;143(2):69–74.
22. Pentheroudakis G, Pavlidis N. Serous papillary peritoneal carcinoma: unknown primary tumour, ovarian cancer counterpart or a distinct entity?—a systematic review. *Crit Rev Oncol Hematol* 2010;75 (1):27–42.
23. Kim HJ, Kim JK, Cho KS. CT features of serous surface papillary carcinoma of the ovary. *AJR Am J Roentgenol* 2004;183(6):1721–1724.
24. Meyers MA. Distribution of intra-abdominal malignant seeding: dependency on dynamics of flow of ascitic fluid. *Am J Roentgenol Radium Ther Nucl Med* 1973;119(1):198–206.
25. Burghardt E, Girardi F, Lahousen M, Tamussino K, Stettner H. Patterns of pelvic and paraaortic lymph node involvement in ovarian cancer. *Gynecol Oncol* 1991;40(2):103–106.
26. Qayyum A, Coakley FV, Westphalen AC, Hricak H, Okuno WT, Powell B. Role of CT and MR imaging in predicting optimal cytoreduction of newly diagnosed primary epithelial ovarian cancer. *Gynecol Oncol* 2005;96(2):301–306.
27. Topuz E, Aydiner A, Saip P, et al. Correlations of serum CA125 level and computerized tomography (CT) imaging with laparotomic findings following intraperitoneal chemotherapy in patients with ovarian cancer. *Eur J Gynaecol Oncol* 2000;21(6): 599–602.
28. Forstner R, Hricak H, Powell CB, Azizi L, Frankel SB, Stern JL. Ovarian cancer recurrence: value of MR imaging. *Radiology* 1995;196(3):715–720.
29. Low RN, Carter WD, Saleh F, Sigeti JS. Ovarian cancer: comparison of findings with perfluorocarbon-enhanced MR imaging, In-111-CYT-103 immunoscintigraphy, and CT. *Radiology* 1995;195(2): 391–400.
30. Ricke J, Sehoul J, Hach C, Hänninen EL, Lichtenegger W, Felix R. Prospective evaluation of contrast-enhanced MRI in the depiction of peritoneal spread in primary or recurrent ovarian cancer. *Eur Radiol* 2003;13(5):943–949.
31. Low RN, Duggan B, Barone RM, Saleh F, Song SY. Treated ovarian cancer: MR imaging, laparotomy reassessment, and serum CA-125 values compared with clinical outcome at 1 year. *Radiology* 2005;235 (3):918–926.
32. Murakami M, Miyamoto T, Iida T, et al. Whole-body positron emission tomography and tumor marker CA125 for detection of recurrence in epithelial ovarian cancer. *Int J Gynecol Cancer* 2006;16 (suppl 1):99–107.
33. Gu P, Pan LL, Wu SQ, Sun L, Huang G. CA 125, PET alone, PET-CT, CT and MRI in diagnosing recurrent ovarian carcinoma: a systematic review and meta-analysis. *Eur J Radiol* 2009;71(1):164–174.
34. Wang ZJ, Boddington S, Wendland M, Meier R, Corot C, Daldrup-Link H. MR imaging of ovarian tumors using folate-receptor-targeted contrast agents. *Pediatr Radiol* 2008;38(5):529–537.
35. Gauden AJ, Phal PM, Drummond KJ. MRI safety; nephrogenic systemic fibrosis and other risks. *J Clin Neurosci* 2010;17(9):1097–1104.
36. Torizuka T, Nobezawa S, Kanno T, et al. Ovarian cancer recurrence: role of whole-body positron emission tomography using 2-[fluorine-18]-fluoro-2-deoxy-D-glucose. *Eur J Nucl Med Mol Imaging* 2002;29(6):797–803.
37. Cho SM, Ha HK, Byun JY, et al. Usefulness of FDG PET for assessment of early recurrent epithelial ovarian cancer. *AJR Am J Roentgenol* 2002;179 (2):391–395.
38. Yen RF, Sun SS, Shen YY, Changlai SP, Kao A. Whole body positron emission tomography with 18F-fluoro-2-deoxyglucose for the detection of recurrent ovarian cancer. *Anticancer Res* 2001;21(5): 3691–3694.
39. Kim CK, Park BK, Choi JY, Kim BG, Han H. Detection of recurrent ovarian cancer at MRI: comparison with integrated PET/CT. *J Comput Assist Tomogr* 2007;31(6):868–875.

40. Zimny M, Siggelkow W, Schröder W, et al. 2-[Fluorine-18]-fluoro-2-deoxy-D-glucose positron emission tomography in the diagnosis of recurrent ovarian cancer. *Gynecol Oncol* 2001;83(2):310–315.
41. Thrall MM, DeLoia JA, Gallion H, Avril N. Clinical use of combined positron emission tomography and computed tomography (FDG-PET/CT) in recurrent ovarian cancer. *Gynecol Oncol* 2007;105(1): 17–22.
42. Sheng XG, Zhang XL, Fu Z, et al. Value of positron emission tomography-CT imaging combined with continual detection of CA125 in serum for diagnosis of early asymptomatic recurrence of epithelial ovarian carcinoma [in Chinese]. *Zhonghua Fu Chan Ke Za Zhi* 2007;42(7):460–463.
43. Soussan M, Wartski M, Cherel P, et al. Impact of FDG PET-CT imaging on the decision making in the biologic suspicion of ovarian carcinoma recurrence. *Gynecol Oncol* 2008;108(1):160–165.
44. Avril N, Sassen S, Schmalfeldt B, et al. Prediction of response to neoadjuvant chemotherapy by sequential F-18-fluorodeoxyglucose positron emission tomography in patients with advanced-stage ovarian cancer. *J Clin Oncol* 2005;23(30):7445–7453.
45. Fulham MJ, Carter J, Baldey A, Hicks RJ, Ramshaw JE, Gibson M. The impact of PET-CT in suspected recurrent ovarian cancer: a prospective multi-centre study as part of the Australian PET Data Collection Project. *Gynecol Oncol* 2009;112(3):462–468.
46. Simcock B, Neesham D, Quinn M, Drummond E, Milner A, Hicks RJ. The impact of PET/CT in the management of recurrent ovarian cancer. *Gynecol Oncol* 2006;103(1):271–276.
47. Sironi S, Messa C, Mangili G, et al. Integrated FDG PET/CT in patients with persistent ovarian cancer: correlation with histologic findings. *Radiology* 2004;233(2):433–440.
48. Majmudar B, Wiskind AK, Croft BN, Dudley AG. The Sister (Mary) Joseph nodule: its significance in gynecology. *Gynecol Oncol* 1991;40(2):152–159.
49. Touraud JP, Lentz N, Dutronc Y, Mercier E, Sagot P, Lambert D. Umbilical cutaneous metastasis (or Sister Mary Joseph's nodule) disclosing an ovarian adenocarcinoma [in French]. *Gynecol Obstet Fertil* 2000;28(10):719–721.
50. Powell FC, Cooper AJ, Massa MC, Goellner JR, Su WP. Sister Mary Joseph's nodule: a clinical and histologic study. *J Am Acad Dermatol* 1984;10(4): 610–615.
51. Salani R, Diaz-Montes T, Giuntoli RL, Bristow RE. Surgical management of mesenteric lymph node metastasis in patients undergoing resectomy for locally advanced ovarian carcinoma. *Ann Surg Oncol* 2007;14(12):3552–3557.
52. Harter P, Gnauert K, Hils R, et al. Pattern and clinical predictors of lymph node metastases in epithelial ovarian cancer. *Int J Gynecol Cancer* 2007;17(6): 1238–1244.
53. Benedetti-Panici P, Greggi S, Maneschi F, et al. Anatomical and pathological study of retroperitoneal nodes in epithelial ovarian cancer. *Gynecol Oncol* 1993;51(2):150–154.
54. Morice P, Joulie F, Camatte S, et al. Lymph node involvement in epithelial ovarian cancer: analysis of 276 pelvic and paraaortic lymphadenectomies and surgical implications. *J Am Coll Surg* 2003;197(2): 198–205.
55. Negishi H, Takeda M, Fujimoto T, et al. Lymphatic mapping and sentinel node identification as related to the primary sites of lymph node metastasis in early stage ovarian cancer. *Gynecol Oncol* 2004;94 (1):161–166.
56. Lorenzen M, Braun J, Gehrckens A, Nicolas V. Value of MRI, CT and findings in staging of gynecologic malignancies [in German]. *Aktuelle Radiol* 1998;8 (6):266–272.
57. Drieskens O, Stroobants S, Gysen M, Vandenbosch G, Mortelmans L, Vergote I. Positron emission tomography with FDG in the detection of peritoneal and retroperitoneal metastases of ovarian cancer. *Gynecol Obstet Invest* 2003;55(3):130–134.
58. Bristow RE, Giuntoli RL 2nd, Pannu HK, Schulick RD, Fishman EK, Wahl RL. Combined PET/CT for detecting recurrent ovarian cancer limited to retroperitoneal lymph nodes. *Gynecol Oncol* 2005;99(2): 294–300.

59. Choi HJ, Roh JW, Seo SS, et al. Comparison of the accuracy of magnetic resonance imaging and positron emission tomography/computed tomography in the presurgical detection of lymph node metastases in patients with uterine cervical carcinoma: a prospective study. *Cancer* 2006;106(4):914-922.
60. Bristow RE, del Carmen MG, Pannu HK, et al. Clinically occult recurrent ovarian cancer: patient selection for secondary cytoreductive surgery using combined PET/CT. *Gynecol Oncol* 2003;90(3): 519-528.
61. Park TW, Kuhn WC. Neoadjuvant chemotherapy in ovarian cancer. *Expert Rev Anticancer Ther* 2004;4 (4):639-647.
62. Kuhn W, Rutke S, Späthe K, et al. Neoadjuvant chemotherapy followed by tumor debulking prolongs survival for patients with poor prognosis in International Federation of Gynecology and Obstetrics Stage IIIC ovarian carcinoma. *Cancer* 2001;92(10): 2585-2591.
63. Fanfani F, Ferrandina G, Corrado G, et al. Impact of interval debulking surgery on clinical outcome in primary unresectable FIGO stage IIIC ovarian cancer patients. *Oncology* 2003;65(4):316-322.
64. Sassen S, Schmalfeldt B, Avril N, et al. Histopathologic assessment of tumor regression after neoadjuvant chemotherapy in advanced-stage ovarian cancer. *Hum Pathol* 2007;38(6):926-934.
65. Lerman H, Metser U, Grisaru D, Fishman A, Lievshitz G, Even-Sapir E. Normal and abnormal 18F-FDG endometrial and ovarian uptake in pre- and postmenopausal patients: assessment by PET/CT. *J Nucl Med* 2004;45(2):266-271.
66. Liu Y. Benign ovarian and endometrial uptake on FDG PET-CT: patterns and pitfalls. *Ann Nucl Med* 2009;23(2):107-112.
67. Subhas N, Patel PV, Pannu HK, Jacene HA, Fishman EK, Wahl RL. Imaging of pelvic malignancies with in-line FDG PET-CT: case examples and common pitfalls of FDG PET. *RadioGraphics* 2005;25 (4):1031-1043.